Radiation Effects on Unsteady Free Convection Heat and Mass Transfer in a Walters-B Viscoelastic Flow Past an Impulsively started Vertical Plate

U. Rajeswara Rao,   V. Ramachandra Prasad,   G. Viswanath,   B. Vasu

Abstract: *A numerical solution of the unsteady radiative, free convection flow with heat and mass transfer of an incompressible viscoelastic fluid past an impulsively started vertical plate is presented here. The Walters-B liquid model is employed to simulate medical cream manufacturing, chemical engineering, and medical biotechnological applications. This rheological model introduces a supplementary terms into the momentum conservation equation. The dimensionless unsteady, coupled and non–linear partial differential conservation equations for the boundary layer regime are solved by an efficient and accurate finite difference scheme of the Crank –Nicolson type. The velocity ,temperature and concentration fields have been studied for the effect of Prandtl number (Pr), Viscoelasticity parameter (Γ), Schmidt number (Sc), Buoyancy ratio parameter (N), Radiation parameter (F). The local skin-friction., Nusselt number and Sherwood number are also presented and analysed graphically. It is also observed that, when the viscoelasticity parameter (Γ) increases, the velocity increases close to the plate surface. An increase in Schmidt number, observed significantly to decrease both velocity and concentration. The present results are compared with available results in literature and are found to be in good agreement.*

Key words: Biotechnology processing; Finite difference method; Heat and Mass transfer; Impulsively started vertical plate; Radiation, Schmidt number; Unsteady viscoelastic flow, Walters–B short memory model.

1. INTRODUCTION:

The flow of a viscous incompressible fluid past an impulsively started infinite vertical plate, moving in its own plane was first studied by Stokes [1]. It is often called Rayleigh's problem in the literature. Such a flow past an impulsively started semi–infinite horizontal plate was first presented by Stewartson [2]. Hall [3] considered the flow past an impulsively started semi- infinite horizontal plate by a finite difference method of a mixed explicit-implicit type. However, Hall analyzed only unsteady velocity field by neglecting the buoyancy effects. Soundalgekar [4] presented an exact solution to the flow of a viscous fluid past an impulsively started infinite isothermal vertical plate. The solution was derived by the Laplace transform technique and the effect of heating or cooling of the plate on the flow field were discussed through Grashof number (Gr). Raptis and Singh [5] studied the flow past an impulsively started infinite vertical plate in a Porous medium by a finite difference method.

The Walters-B viscoelastic model [6] was developed to simulate viscous fluids possessing short memory elastic effects and can simulate accurately many complex polymeric, biotechnological and tribiological fluids. The Walters-B model has therefore been studied extensively in many flow problems. Das et al [7] considered the mass transfer effects on the flow past an impulsively started infinite vertical plate with a constant mass flux and chemical reaction. Muthucumaraswamy and Ganesan[8] studied, The unsteady flow past an impulsively started isothermal vertical plate with mass transfer by an implicit finite difference method. Muthucumaraswamy and Ganesan [9, 10] solved the problem of unsteady flow past an impulsively started vertical plate with uniform heat and mass flux, and variable temperature and mass flux respectively. In this context of space technology and in processes involving high temperatures and the effects of radiation are of the vital importance.

———————————————

- *U. Rareswara Rao, Professor, Dept of Mathematics, Sri Krishnadevaraya Universiy,Anantapur-515003, India.*
- *V. R. Prasad, Professor, Dept. of Mathematics, Madanapalle Institute of Technology and Science, Madanapalle-517325, India. Email:rcpmaths@gmail.com*
- *G. Viswanath, Assoc. Professor,Dept. of Mathematics, Anantha Lakshmi Institute of Technology and Sciences, Anantapur-515721, India. Email: visu.gudipati@gmail.com.*
- *B. Vasu, Associate Professor, Dept. of Mathematics, Madanapalle Institute of Technology and Science, Madanapalle-517325, India. Email: bvsmaths1@gmail.com.*

———————————————

Recent developments in hypersonic flights, missile re-entry, rocket combustion chambers power plants for inter-planetary flight and gas cooled nuclear reactors focused attention on thermal radiation as a mode of energy transfer, and emphasize the need for improved understanding of radiative transfer in these processes. The interaction of radiation with laminar free convection heat transfer from a vertical plate was investigated by Cess [11] for an absorbing, emitting fluid in the optically thick region , using the singular perturbation technique. Arpaci [12] considered a similar problem in both the optically thin and optically thick regions and used approximate integral technique and first order profiles to solve the energy equation.Cheng et al [13] studied a related problem for an absorbing, emitting and isotropically scattering fluid, and treated the radiation part of the problem exactly with the normal mode expansion technique. Raptis [14] analyzed both the thermal radiation and free convection flow through a porous medium by using a perturbation technique. Hossain and Takhar [15] studied the radiation effects on mixed convection along a vertical plate with the uniform surface temperature using the Keller Box finite difference method. In all these papers, the flow taken steady, Mansour [16] studied the radiative and and free convection effects on the oscillatory flow past a vertical plate. Raptis and Perdikis [17] considered the problem of thermal radiation and free convection flow past moving plate. Das et al [18] analyzed the radiation effects on the flow past an impulsively started infinite isothermal vertical plate, the governing equations are solved by using Laplace transform technique. Chang et al [19] analyzed the unsteady buoyancy-driven flow and species diffusion in a Walters-B viscoelastic flow along a vertical plate with transpiration effects. They showed that the flow is accelerated with a rise in viscoelasticity parameter with both time and locations close to the plate surface and increasing Schmidt number(Sc) suppresses both velocity and concentratio in time whereas increasing species Grashof number (buoyancy parameter) accelerates flow through time. V. Prasad et al [20] studied Radiation and mass transfer effects on two-dimensional flow past an impulsively started infinite vertical plate. Observed when radiation parameter increases, velocity, temperature decreases and time taken to reach steady state increases.

The aim of the present paper is to analyze the radiation effects on an unsteady two-dimensional laminar simultaneous free convection heat and mass transfer in a Walters -B viscoelastic flow past an impulsively started vertical plate. The equations of continuity, linear momentum, energy and diffusion, which govern the flow field, are solved by using an implicit finite difference method of The Crank–Nicolson type. The behavior of the velocity, temperature, concentration, skin-friction and Sherwood number has been

discussed for variations in the governing parameters. Here the results analyzed graphically.

1.1. CONSTITUTIVE EQUATIONS FOR THE WALTERS-B VISCOELASTIC FLUID:

The Walters-B viscoelastic model (Walters-1962) was developed to simulate viscous fluids possessing short memory elastic effects and can simulate accurately many complex polymeric, biotechnological and tribiological fluids. Walters-B model has therefore been studied extensively in many flow problems .This model has been shown to capture the characteristics of the viscoelastic polymer Solutions, hydro-carbons, paints and other chemical engineering fluids. The Walters-B model generates highly non-linear flow equations which are an order higher than the classical Navier–Stokes (Newtonian) equations. It also incorporates elastic properties of the fluids are important in extensional behavior of polymers. The constitute equations for a Walters-B liquid in tensorial form may be represented as follows:

$$p_{ik} = -pg_{ik} + p_{ik}^* \tag{1.1}$$

$$p_{ik}^* = 2\int_{-\infty}^{t} \Psi(t-t')e_{ik}^{(1)}(t^*)dt^* \tag{1.2}$$

$$\Psi(t-t^*) = \int_{0}^{\infty} \frac{N(\tau)}{\tau} e^{\frac{-(t-t^*)}{t}} d\tau \tag{1.3}$$

Where p_{ik} is the stress tensor, p is arbitrary isotropic pressure, g_{ik} is the metric tensor of fixed coordinate system X_i, $e_{ik}^{(1)}$ is the rate of strain tensor and $N(\tau)$ is the distribution function of relaxation time τ .The following generalized form of (2) has been shown by Walters to be valid for all classes of motion and stress.

$$p^{*ik}(x,t) = 2\int_{-\infty}^{t} \Psi(t-t')\frac{\partial x^i}{\partial x^{*m}}\frac{\partial x^k}{\partial x^{*r}} e^{(1)mr}(x^*t^*)dt^* \tag{1.4}$$

In which $x_i^* = x_i^*(x,t,t^*)$ denotes the position at time t^* of the element which is instantaneously at the position x_i at time t. Liquids obeying the relations (1) and (4) are of the Walters –B type. For such fluids with memory i.e. low relaxation times, equation (4) may be simplified to:

$$p^{*ik}(x,t) = 2\eta_0 e^{(1)ik} - 2k_0 \frac{\partial e^{(1)ik}}{\partial t} \tag{1.5}$$

In which $\eta_0 = \int_{0}^{\infty} N(\tau) d\tau$ defines the limiting Walters-B viscosity at low shear rates, $k_0 = \int_{0}^{\infty} \tau N(\tau)d\tau$ is the Walters-B visco-elasticity parameter and $\frac{\partial}{\partial t}$ is the convicted time derivative. This rheological model is very versatile and robust, gives a relatively simple mathematical formulation which is easily incorporated into boundary layer theory for engineering applications.

2. MATHEMATICAL ANALYSIS:

An unsteady two–dimensional laminar natural convection radiative flow of a viscoelastic fluid past an Impulsively started vertical plate is considered. The x- axis is taken along the plate in the upward direction and y-axis is taken normal to it. The physical model is shown in fig. 1.
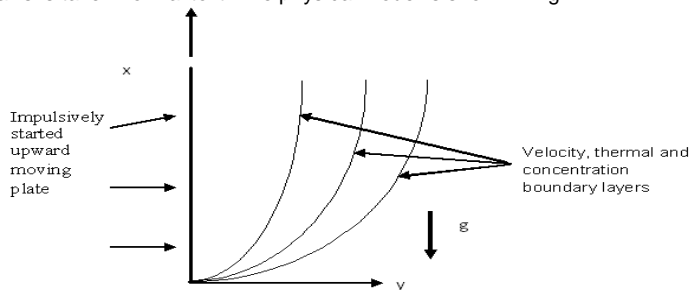

Fig. 1 Physical model and coordinate system

Initially assumed that the plate and the fluid are at the same temperature T'_∞ and concentration level C'_∞ everywhere in the fluid. At the time $t' > 0$ the temperature of plate and concentration level near the plate are raised to T'_w and C'_w respectively and are maintained constantly thereafter. It is assumed that the concentration C' of the diffusing species in the mixture is very less in comparison to the other chemical species, which are present and hence the Soret and Dufour effects are negligible. It is also assumed that there is no chemical reaction between the diffusing species and the fluid. Under the above assumptions, the governing boundary layer equations with Boussinesq's approximation are:

$$\frac{\partial u}{\partial x} + \frac{\partial v}{\partial y} = 0 \tag{2.1}$$

$$\frac{\partial u}{\partial t'} + u\frac{\partial u}{\partial x} + v\frac{\partial u}{\partial y} = g\beta(T'-T'_\infty) + g\beta^*(C'-C'_\infty) + \nu\frac{\partial^2 u}{\partial y^2} - k_0\frac{\partial^3 u}{\partial y^2 \partial t'} \tag{2.2}$$

$$\frac{\partial T'}{\partial t'} + u\frac{\partial T'}{\partial x} + v\frac{\partial T'}{\partial y} = \alpha\frac{\partial^2 T'}{\partial y^2} - \frac{1}{\rho c_p}\frac{\partial q_r}{\partial y} \tag{2.3}$$

$$\frac{\partial C'}{\partial t'} + u\frac{\partial C'}{\partial x} + v\frac{\partial C'}{\partial y} = D\frac{\partial^2 C'}{\partial y^2} \tag{2.4}$$

The initial and boundary conditions are:

$t' \le 0 : u = 0, v = 0, T' = T'_\infty, C' = C'_\infty$

$t' > 0 : u = u_0, v = 0, T' = T'_w, C' = C'_w \quad at \ y = 0 \tag{2.5}$

$u = 0, \ T' = T'_\infty, C' = C'_\infty, \quad at \ x = 0$

$u \to 0, T' \to T'_\infty, C' \to C'_\infty \quad as \ y \to \infty$

By using the Rosseland approximation the radiative heat flux q_r is given by

$$q_r = -\frac{4\sigma_s}{3k_e}\frac{\partial T'^4}{\partial y} \tag{2.6}$$

Where σ_s is the Stefan -Boltzmann constant and k_e the mean absorption coefficient? It should be noted that by using the Rosseland approximation, the present analysis is limited to optically thick fluids. If temperature differences within the flow are significantly small, then equation [11] can be linearised by expanding T'^4 into the Taylor series about T'_∞, which after neglect higher order terms takes the form:

$$T'^4 \cong 4T'^3_\infty T' - 3 T'^4_\infty \tag{2.7}$$

In view of equations [11] and [12], eqn. [8] reduces to

$$\frac{\partial T'}{\partial t'} + u\frac{\partial T'}{\partial x} + v\frac{\partial T'}{\partial y} = \alpha\frac{\partial^2 T'}{\partial y^2} + \frac{16\,\sigma_s T'^3_\infty}{3k_e\rho c_p}\frac{\partial^2 T'}{\partial y^2} \tag{2.8}$$

On introducing the following non-dimensional quantities:

$$X = \frac{xu_o}{\nu}, \quad Y = \frac{yu_o}{\nu}, U = \frac{u}{u_o}, \quad V = \frac{v}{u_o}, \quad T = \frac{T'-T'_\infty}{T'_w-T'_\infty},$$

$$t = \frac{t'u_o^2}{\nu}, \quad \Gamma = \frac{k_o u_o^2}{\nu^2}, \quad C = \frac{C'-C'_\infty}{C'_w-C'_\infty}, \quad Gm = \frac{\nu g\beta^*(C'_w-C'_\infty)}{u_o^3} \tag{2.9}$$

$$F = \frac{k_e k}{4\sigma_s T'^3_\infty}, \quad Gr = \frac{\nu g\beta(T'_w-T'_\infty)}{u_o^3}, \quad Pr = \frac{\nu}{\alpha},$$

$$Sc = \frac{\nu}{D}, \quad \nu = \frac{\mu}{\rho}, \quad \frac{1}{Pr} = \frac{k}{\mu c_p}.$$

Equations (2.1), (2.2), (2.3), and (2.4) are reduced under the boundary conditions to the following non-dimensional form:

$$\frac{\partial U}{\partial X} + \frac{\partial U}{\partial Y} = 0 \tag{2.10}$$

$$\frac{\partial U}{\partial t} + U\frac{\partial U}{\partial X} + V\frac{\partial U}{\partial Y} = \frac{\partial^2 U}{\partial Y^2} + Gr.T + Gm.C - \Gamma\frac{\partial^3 U}{\partial Y^2 \partial t} \tag{2.11}$$

$$\frac{\partial T}{\partial t} + U\frac{\partial T}{\partial X} + V\frac{\partial T}{\partial Y} = \frac{1}{Pr}\left[1 + \frac{4}{3F}\right]\frac{\partial^2 T}{\partial Y^2} \tag{2.12}$$

$$\frac{\partial C}{\partial t} + U\frac{\partial C}{\partial X} + V\frac{\partial C}{\partial Y} = \frac{1}{Sc}\frac{\partial^2 C}{\partial y^2} \tag{2.13}$$

The corresponding initial and boundary conditions are:
$$t \leq 0 : U = 0, V = 0, T = 0, C = 0$$

$$t > 0: U = 1, V = 0, T = 1, C = 1 \quad at \quad y = 0 \tag{2.14}$$

$$U = 0, T = 0, C = 0, \quad at \ X = 0$$

$$U \to 0, T \to 0, C \to 0 \quad as \ Y \to \infty$$

L–is the length of the plate, Gr-the Grashof number Pr–the Prandtl number, Sc-Schmidt number, F- the radiation parameter, N-the buoyancy ratio parameter, Γ- visco-elasticity parameter. Knowing the velocity, temperature, and concentration fields, it is interesting to find local Skin-friction, Nusselt number and Sherwood numbers in non dimensional equation model, computed with the following mathematical expressions.

$$\tau_X = Gr^{\frac{3}{4}}\left(\frac{\partial U}{\partial Y}\right)_{Y=0} \tag{2.15}$$

$$Nu_X = \frac{-X\,Gr^{\frac{1}{4}}\left(\frac{\partial T}{\partial Y}\right)_{Y=0}}{T_{Y=0}} \tag{2.16}$$

$$Sh_X = \frac{-X\,Gr^{\frac{1}{4}}\left(\frac{\partial C}{\partial Y}\right)_{Y=0}}{C_{Y=0}} \tag{2.17}$$

When $\Gamma \to \infty$, the dimensionless equations (2.10), (2.11), (2.12) and (2.13) under conditions (2.14) reduces to Newtonian flow.

3. NUMERICAL TECHNIQUE:

In order to solve these unsteady, non-linear coupled equations (2.10), (2.11), (2.12) and (2.13) under the conditions (2.14), an implicit finite difference scheme of Crank-Nicolson type has been employed. The region of integration is considered as a rectangle with sides $X_{max}(= 1)$ and $Y_{max}(= 14)$, where Y_{max} corresponds to $Y = \infty$, which lies very well outside the momentum, energy and concentration boundary layers. The finite difference equations are:

$$\frac{\left[U_{i,j-1}^{n+1} - U_{i-1,j-1}^{n+1} + U_{i,j}^{n+1} - U_{i-1,j}^{n+1} + U_{i,j-1}^{n} - U_{i-1,j-1}^{n} + U_{i,j}^{n} - U_{i-1,j}^{n}\right]}{4\Delta X}$$

$$+\frac{\left[V_{i,j}^{n+1} - V_{i,j-1}^{n+1} + V_{i,j}^{n} - V_{i,j-1}^{n}\right]}{2\Delta Y} = 0 \tag{3.1}$$

$$\frac{\left[U_{i,j}^{n+1} - U_{i,j}^{n}\right]}{\Delta t} + U_{i,j}^{n}\frac{\left[U_{i,j}^{n+1} - U_{i-1,j}^{n+1} + U_{i,j}^{n} - U_{i-1,j}^{n}\right]}{2\Delta X}$$

$$+ V_{i,j}^{n}\frac{\left[U_{i,j+1}^{n+1} - U_{i,j-1}^{n+1} + U_{i,j+1}^{n} - U_{i,j-1}^{n}\right]}{4\Delta Y} =$$

$$\frac{\left[U_{i,j-1}^{n+1} - 2U_{i,j}^{n+1} + U_{i,j+1}^{n+1} + U_{i,j-1}^{n} - 2U_{i,j}^{n} + U_{i,j+1}^{n}\right]}{2(\Delta Y)^2} +$$

$$Gr.\frac{\left[T_{i,j}^{n+1} + T_{i,j}^{n}\right]}{2} + Gm.\frac{\left[C_{i,j}^{n+1} + C_{i,j}^{n}\right]}{2}$$

$$-\Gamma\frac{\left[U_{i,j-1}^{n+1} - 2U_{i,j}^{n+1} + U_{i,j+1}^{n+1} + U_{i,j-1}^{n} - 2U_{i,j}^{n} + U_{i,j+1}^{n}\right]}{2(\Delta Y)^2\Delta t} \tag{3.2}$$

$$\frac{\left[T_{i,j}^{n+1} - T_{i,j}^{n}\right]}{\Delta t} + U_{i,j}^{n}\frac{\left[T_{i,j}^{n+1} - T_{i-1,j}^{n+1} + T_{i,j}^{n} - T_{i.1,j}^{n}\right]}{2\Delta X} +$$

$$+V_{i,j}^{n}\frac{\left[T_{i,j+1}^{n+1} - T_{i,j-1}^{n+1} + T_{i,j+1}^{n} T_{i,j-1}^{n}\right]}{4\Delta Y} =$$

$$\frac{1}{Pr}\left[1 + \frac{4}{3F}\right]\frac{\left[T_{i,j-1}^{n+1} - 2T_{i,j}^{n+1} + T_{i,j+1}^{n+1} + T_{i,j-1}^{n} - 2T_{i,j}^{n} + T_{i,j+1}^{n}\right]}{2(\Delta Y)^2} \tag{3.3}$$

$$\frac{\left[C_{i,j}^{n+1} - C_{i,j}^{n}\right]}{\Delta t} + U_{i,j}^{n}\frac{\left[C_{i,j}^{n+1} - C_{i-1,j}^{n+1} + C_{i,j}^{n} - C_{i-1,j}^{n}\right]}{2\Delta X}$$

$$+ V_{i,j}^{n}\frac{\left[C_{i,j+1}^{n+1} - C_{i,j-1}^{n+1} + C_{i,j+1}^{n} - C_{i,j-1}^{n}\right]}{4\Delta Y} =$$

$$\frac{\left[C_{i,j-1}^{n+1} - 2C_{i,j}^{n+1} + C_{i,j+1}^{n+1} + C_{i,j-1}^{n} - 2C_{i,j}^{n} + C_{i,j+1}^{n}\right]}{2\,Sc\,(\Delta Y)^2} \tag{3.4}$$

The region of integration is considered as a rectangle with side $X_{max}(= 1)$ and $Y_{max}(= 14)$ Where Y_{max} corresponds to $Y = \infty$, which lies very well outside the momentum, energy and concentration boundary layers. After some preliminary numerical experiments the mesh sizes have been fixed as $\Delta X = 0.05$, $\Delta Y = 0.25$ with time step $\Delta t = 0.01$. During any one time step, the coefficients $U_{i,j}^{n+1}$ and $V_{i,j}^{n+1}$ appearing in the difference equations are treated as constants. Here i designates the grid point along the x-direction, j-along the y-direction. The values of C, T, U and V are known at all grid points when t = 0.

The finite difference equations at every internal nodal point on a particular i level constitutes a tridiagonal system of equations and is solved by using Thomas algorithm. Thus the values of C are known at every nodal point at a particular i-level at (n+1)[th] time level. In a similar way computations are carried out by moving along i-direction. After computing values corresponding to each i at a time level, the values at the next time level are determined in a similar manner. Computations are repeated until the steady state is reached. Here the steady state solution is assumed to have reached when the absolute difference between the values of the velocity U, temperature T, as well as the concentration C at two consecutive time steps are less than 10^{-5} at all grid points.
The derivatives involved in [15],[16],[17] and[18] are evaluated using five-point approximation formula and the integrals are evaluated using Newton- Cotes closed integration formula.

4. RESULTS AND DISCUSSION:

A representative set of numerical results is shown graphically in Figures, to illustrate the influence of physical parameters, viz., viscoelasticity parameter (Γ) = 0.005, thermal Grashof parameter (Gr) = 1.0, species Grashof parameter (Gm) = 1.0, Schmidt number (Sc) = 0.25 (oxygen diffusing in the viscoelastic fluid),radiation parameter(F) = 0.5 and Prandtl number (Pr) = 0.71 (water-based solvents). All graphs therefore correspond to these values unless specifically otherwise indicated.

we have presented the variation of velocity (U), temperature function (T) and concentration (C) versus (Y) with on viscoelasticity (Γ) at X = 1.0. An increase in Γ from 0 to 0.001, 0.003, 0.005 and the maximum value of 0.007,

as depicted in fig. **2(a)**, clearly enhances the velocity, *U* which ascends sharply and peaks in close vicinity to the plate surface (*Y* = 0). With increasing distance from the plate wall however the velocity *U* is adversely affected by increasing viscoelasticity i.e. the flow is decelerated. The switchover in behavior corresponds to approximately *Y* = 1. With increasing (Y) velocity profiles decay smoothly to zero in the free stream at the edge of the boundary layer. The opposite effect is caused by an increase in time. A rise in t from 3.69 through 3.54, 3.72 4.98 to 5.42 causes a decrease in flow velocity, U nearer the wall in this case the maximum velocity arises for the least time progressed. fig. **2(b)** increasing viscoelasticity Γ is seen to decrease temperature throughout the boundary layer. The graphs show therefore that increasing viscoelasticity cools the flow. With progression of time, however the temperature, *T* is consistently enhanced i.e. the fluid is heated as time progresses. A similar response is observed for the concentration field, *C*, in fig. **2(c),** Increasing viscoelasticity again reduces concentration, showing that species diffuses more effectively in Newtonian fluids (Γ = 0) than in strongly viscoelastic fluids. Once again with greater elapse in time the concentration values are reduced throughout the boundary layer regime (0 < *Y*< 14).

To illustrate the effect of Prandtl number, Pr and time, t on velocity U, temperature T, and concentration C. Increasing Pr clearly reduces strongly velocity, *U* [figure **3(a)**] both in the near-wall regime and the far-field regime of the boundary layer. Velocity is therefore maximized when Pr = 0.3 (minimum) and minimized for the largest value of Pr (10.0). *Pr* defines the ratio of momentum diffusivity (ν) to thermal diffusivity. *Pr* < 1 physically corresponds to cases where heat diffuses faster than momentum. *Pr* = 0.71 is representative of water-based solvents and Pr >>1. An increase in time, t, also serves to strongly retard the flow. With increasing Pr from 0.3 through 0.7, 1.0, 5.0 to 10.0, temperature, *T* as shown in fig. **3(b)**, is markedly reduced throughout the boundary layer. Our computations show that a rise in *Pr* depresses the temperature function. For the case of *Pr* = 1, thermal and velocity boundary layer thicknesses are equal. Conversely the concentration values [figure **3(c)**] are slightly increased with a rise in *Pr* from 0.3 through intermediate values to 10. However with progression of time the concentration is found to be decreased in the boundary layer regime.

The distributions of velocity (*U*) and concentration (*C*) versus coordinate (*Y*) for various Schmidt numbers (*Sc*) and time (*t*), close to the leading edge at *X* = 1.0, are shown. These figures again correspond to a viscoelasticity parameter Γ=0.005 i.e weak elasticity and strongly viscous effects. An increase in Sc from 0.1 (low weight diffusing gas species) through 0.5 (oxygen diffusing) to 1.0 (denser hydrocarbon derivatives as the diffusing species), 3.0 and 5.0, clearly strongly decelerates the flow. In Fig. **4(a),** the maximum velocity arises at Sc = 0.1 very close to the wall. All profiles then descend smoothly to zero in the free stream. With higher Sc values the gradient of velocity profiles is lesser prior to the peak velocity but greater after the peak. An increase in time, *t*, is found to accelerate the flow. Conversely the temperature values [figure **4(b)**] are slightly increased with a rise in *Sc* from 0.1 through intermediate values to 0.6. However with progression of time the temperature is found to be decreased in the boundary layer regime. Figure **4(c)** shows that increase in *Schmidt number effectively* depresses concentration values in the boundary layer regime since higher *Sc* values will physically manifest in a decrease of molecular diffusivity (*D*) of the viscoelastic fluid.

It is of great interest to show how the radiation-conduction interaction effects on velocity, temperature and concentration. It is observed that, initially for lower values of the radiation parameter F, the heat transfer is dominated by conduction, as the values of F increases the radiation absorption in boundary layer increases. i.e., an increase in the radiation parameter F from 0.1 through 0.5, 1.0, 3.0, 5.0 and 10.0 results in a decrease in the temperature and increase in concentration shown in figs. **5(b)** and **5(c)**.Here the velocity profiles increases initially and then slowly decreases to zero due to viscoelasticity shown in fig. **5(a)**.

The effects of thermal Grashof number Gr are shown in Figs. Figure **6(a)** indicates that an increasing Gr from 0.1 through 1, 2, 4 to 6 strongly boosts velocity in particular over the zone 0 < Y < 2. There is a rapid rise in the velocity near the wall especially for the cases Gr = 4 and Gr = 6. Peak value of Gr = 6 is about $Y \sim 0.75$ the profiles generally descend smoothly towards zero

although the rate of descend is greater corresponding to higher thermal Grashof numbers. Gr defines the ratio of thermal buoyancy force to the viscous hydrodynamic force and as expected does accelerate the flow. Temperature distribution T versus Y is plotted in figure **6(b)** and is seen to decrease with a rise in thermal Grashof number, results which agree with fundamental studies on free convection (Schlichting boundary layer theory). Increasing Gr values figure **6(c)** are seen to considerably reduce concentration function values (C) throughout the boundary layer.

Velocity U, is observed to increase considerably with rise in Gm from 0.1 to 6. Hence species Grashof number boosts velocity of the fluid indicating that buoyancy as an accelerating effect on the flow field. All temperatures descend from unity at the wall to zero in the free stream. The depression in temperature is maximized by larger species Grashof number in the vicinity $Y \sim 2.1$, indicating a similar trend to the influence of thermal Grashof number [fig.**7 (b)**]. Dimensionless concentration, C as depicted in figure **7(c)**, is also seen to be reduced by increasing the species Grashof number. All profiles decay smoothly from unity at the vertical surface to zero as $y \rightarrow \infty$.

The variation of dimensionless local skin friction (surface shear stress), τ_x, Nusselt number (surface heat transfer gradient), Nu_x and the Sherwood number (surface concentration gradient), Sh_x, versus axial coordinate (*X*) for various viscoelasticity parameters (Γ) and time (*t*) are illustrated. Shear stress is clearly enhanced with increasing viscoelasticity (i.e. stronger elastic effects) i.e. the flow is accelerated, a trend consistent with our earlier computations in figure **8(a)**. The ascent in shear stress is very rapid from the leading edge (*X*= 0) but more gradual as we progress along the plate surface away from the plane. With an increase in time, *t*, shear stress, τ_x, is however increased. Increasing viscoelasticity (Γ) is observed in figure **8(b)** to enhance local Nusselt number, Nu_x values whereas they are again decreased with greater time. Similarly in figure 8(c), the local Sherwood number Sh_x values are elevated with an increase in elastic effects i.e. a rise in Γ from 0 (Newtonian flow) through 0.001, 0.003 to 0.005 but depressed finally in slightly with time. The influence of Radiation parameter (F) and time (t) on τ_x, Nu_x and Sh_x, versus axial coordinate (*X*) are depicted. An increase in F from 0.1 through 0.5, 1, 3 to 5, strongly increases both τ_x and Nu_x along the entire plate surface i.e. for all X. However with an increase in time (*t*) both shear stress and local Nusselt number are enhanced. With increasing *F* values, local Sherwood number, Sh_x, as shown in figure **9(c)**, is boosted considerably along the plate surface; gradients of the profiles are also found to diverge with increasing *X* values. However an increase in time, *t*, serves to reduce local Sherwood numbers.

5. CONCLUSIONS:

A two-dimensional, unsteady laminar incompressible boundary layer model has been presented for the external flow, heat and mass transfer in a Walters-B viscoelastic buoyancy-driven radiative flow from an impulsively started vertical plate. The Walters-B viscoelastic model has been employed which is valid for short memory polymeric fluids. The dimensionless conservation equations have been solved with the well-tested, robust, highly efficient, implicit Crank Nicolson finite difference numerical method. The present computations have shown that increasing viscoelasticity accelerates the velocity and enhances shear stress (local skin friction), local Nusselt number and local Sherwood number, but reduces temperature and concentration in the boundary layer. Here the radiation effects on flow. Initially for lower values of the radiation parameter F, the heat transfer is dominated by conduction, as the values of F increases the radiation absorption in boundary layer increases. i.e., an increase in the radiation parameter F results, decrease in the temperature and increase in concentration. This phenomenon is of interest in very high temperature (e.g. glass) flows in the mechanical and chemical process industries and is currently under investigation.

NOMENCLATURE:

x, y Coordinates along the plate generator and normal

to the generator respectively

u, v Velocity components along X, Y directions respectively

g Acceleration due to gravity

c_p Specific heat at constant pressure

C' The species concentration in the boundary layer

C Dimensionless concentration

D Mass diffusion coefficient

Gr Thermal Grashof number

Gm Mass Grashof number

k Thermal conductivity

L Reference length

N Buoyancy ratio parameter

F Radiation parameter

Nu_x Dimensionless local Nusselt number

Pr Prandtl number

Sc Schmidt number

Sh_x Dimensionless local Sherwood number

T' Temperature

T Dimensionless temperature

t' Time

t Dimensionless time

k_0 Walters-B viscoelasticity parameter

u_0 Velocity of the plate

U, V Dimensionless velocity components in X, Y directions respectively

Greek symbols:

α Thermal diffusivity

β Volumetric coefficient of thermal expansion

β^* Volumetric coefficient of expansion with concentration

ν Kinematic viscosity

ρ Density

Γ Viscoelastic parameter

Δt Dimensionless time-step in X-direction

ΔX Dimensionless finite difference grid size

ΔY Dimensionless finite difference grid size in Y-direction

τ_x Dimensionless local skin-friction

Subscripts:

w Conditions on the wall

∞ Free stream condition

REFERENCES:

[1]. Stokes G.G(1995), On the effect of internal friction of fluids on the motion of pendulums, *Cambridge Phil. Trans.,* Vol. IX, pp. 8-106.

[2]. Stewartson, K., On the impulsive motion of a flat plate in a viscous fluid *Quart. J. Mech. Appl. Mathematics*, 4 (1951), pp. 182-198.

[3].Hall M.G.(1969),Boundary layer over an Impulsively started flat plate, *Proc.yal Soc.,London,* Vol.310A, pp.414.

[4]. Soundalgekar, V.M.,(1977) Free convection and mass transfer effects on the viscoelastic flow past an impulsively-started vertical plate, *ASME J. Applied Mechanics*, 46 (1979), pp. 757-760.

[5]. Raptis. A and Singh. A. K (1985), free convection flow past an impulsively started vertical plate in a porous medium by finite difference method. *Astro physics and Space Science.* Vol. 112, pp. 259-265.

[6] K. Walters, non-Newtonian effects in some viscoelastic liquids whose behavior at small ratesof shear is characterized by a general linear equations of state, *Quart. J. Mech. Applied Math*, 15(1962), 6. pp. 63-76.

[7]. Das U . N., Deka R.K and V. M. Soundalgekar (1994) studied, the mass transfer effects onthe flow past an impulsively started infinite vertical plate with a constant mass flux and chemical reaction. *J. of Theo. Appl. Fluid Mech* , 1 (2)(1996) 111-115.

[8]. R.Muthucumaraswamy. P.Ganesan, Unsteady flow past an impulsively started semi–infinite vertical plate with heat and mass transfer, *J. of heat and mass trans*., 34(1998), pp187-193.

[9].Muthucumaraswamy.R. and Ganesan. P.(2001) studied the the first order chemical reaction onflow past an impulsively started vertical plate with uniform heat and mass flux Acta. Mech. Vol. 147, pp.45-47.

[10]. Muthucumaraswamy.R. and Ganesan. P. (1999) Flow past an impulsively started vertical plate with variable temperature and mass flux. *J.Of Heat and Mass Transfer,*Vol.34, pp.487-493.

[11]. Cess R .D. , The interaction of thermal radiation with free convection heat and mass transfer*. Int .J .of heat and mass transfer* 9 (1966) pp 1269 - 1277.

[12]. Vedat S.Arpaci(1968), effect if thermal radiation on the laminar free convection from a heatedvertical plate , *Int. J. Heat and Mass Transfer,* Vol. 11, pp.871-881.

[13].Cheng E.H. and Ozisik M.N (1972), Radiation with free convection in an absorbing, emitting and scattering medium. *Int. J. Heat and Mass Transfer,* Vol. 15, pp.1243-1252.

[14].Raptis. A. (1998) Radiation and free convection flow through a porous medium, *Int.Commun. Heat and Mass transfer ,* Vol. 25, pp.289-295.

[15].Hossain. M. A. And Takhar H.S (1996), Radiation effect on mixed convection along a vertical plate with uniform surface temperature, *Heat mass transfer* , Vol.31, pp. 243-248.

[16]. Mansour. M. H. (1990) Radiative and free convection effects on the oscillatory flow past a vertical plate. *Astro physics and Space Science,* Vol. 166, pp. 26-75.

[17] Raptis .A. and Perdikis .C (1999), Radiation and free convection flow past a moving plate. *Appl. Mech.Eng.*, Vol. 4, pp. 817-821.

[18] U .N. Das, R. Deka and V. M. Soundalgekar studied, The radiation effects on flow past an Impulsively started infinite vertical plate. *J. of Theo. Appl. Fluid Mech* , 1 (2)(1996) 111-115.

[19]. T. B .Chang Beg, O. Anwar and M. Narahari analysed, the unsteady buoyance-driven flow and species diffusion in a Walters-B viscoelastic flow along a vertical plate with transition effects. *J. Theoretical Applied Mechanics*, review (2009).

[20] V. R. Prasad, N. Bhaskar Reddy and R. Muthucumaraswamy, Radiation and mass transfer effects on two-dimensional flow past an impulsively started infinite vertical plate. *Int. J. of Thermal Sciences*, 46, 12 (2007), pp.1251-1258.

[21]. Chamkha A . J., Takhar. H S , analysed, The effects of radiation on free convection flow past a semi-infinite vertical plate with mass transfer. *Chem. Eng. J* .Vol .84(2001),pp.335-342.

[22]. A . A .Raptis and H .S. Takhar studied, Flate thermal convection boundary layers flow of a Walters-B fluid usig numerical shooting quadrature. *Int . Comm. Heat and Mass Transfer.* 16, (1989) , 2, pp. 193 - 197.

[23]Frank.P.andDawitt.P.Dewitt.,Fundamentals of heat and mass transfer, *Fifth edition, Jhon Wiley*, 2007.
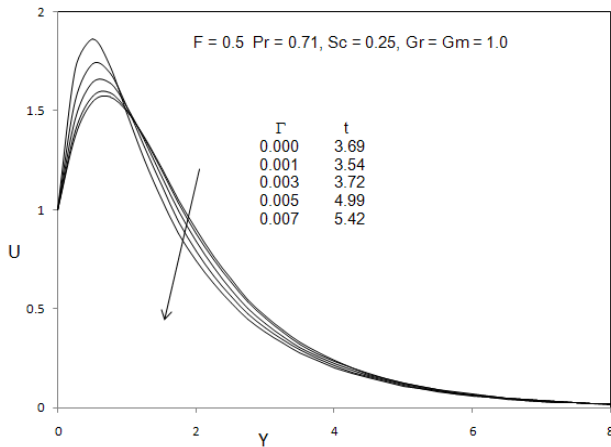
GRAPHS:

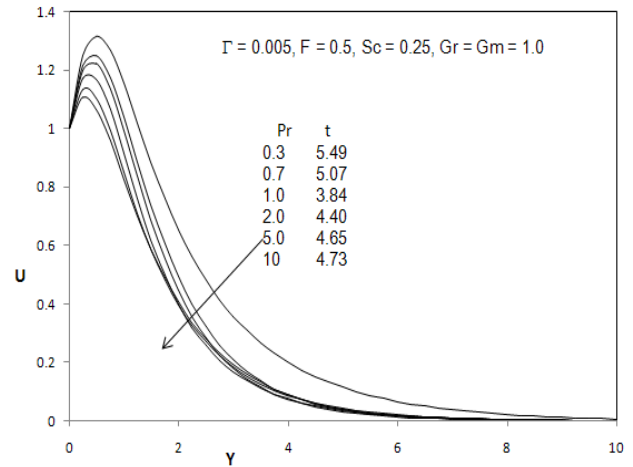Fig 2(a) Steady state velocity profiles at X = 1.0 for different Γ

Fig 3(a) Steady state velocity profiles at X = 1.0 for different Pr
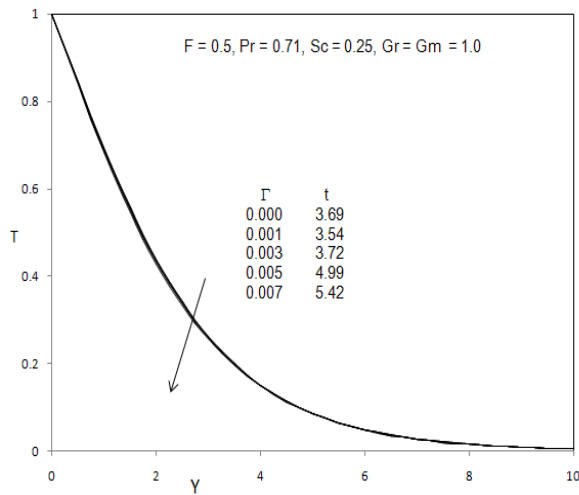

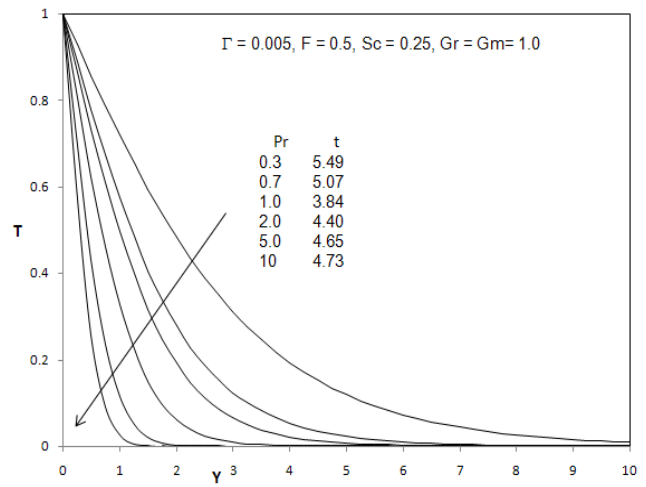Fig 2(b) Steady state concentration profiles at X = 1.0 for different Γ

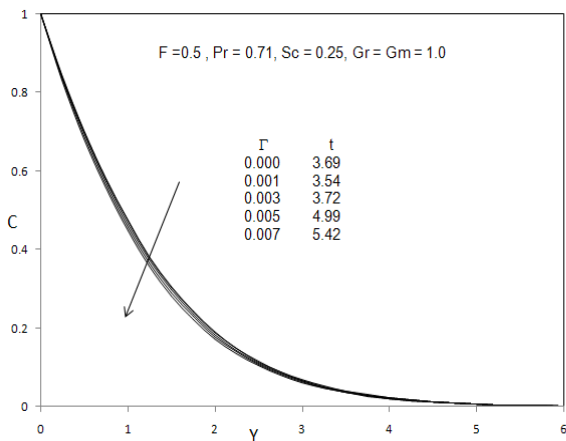Fig 3(b) Steady state temperature profiles at X = 1.0 for different Pr

Fig 2(c) Steady state concentration profiles at X = 1.0 for different Γ
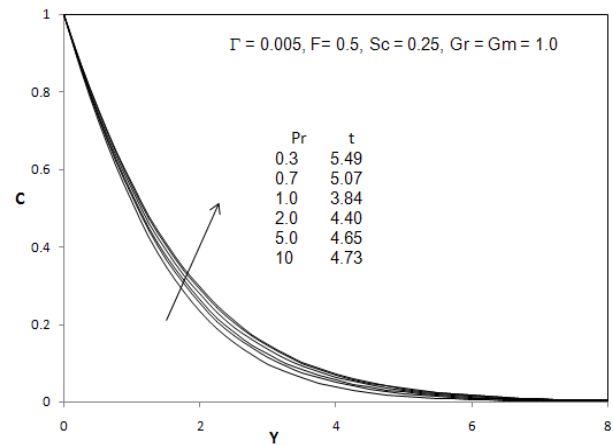

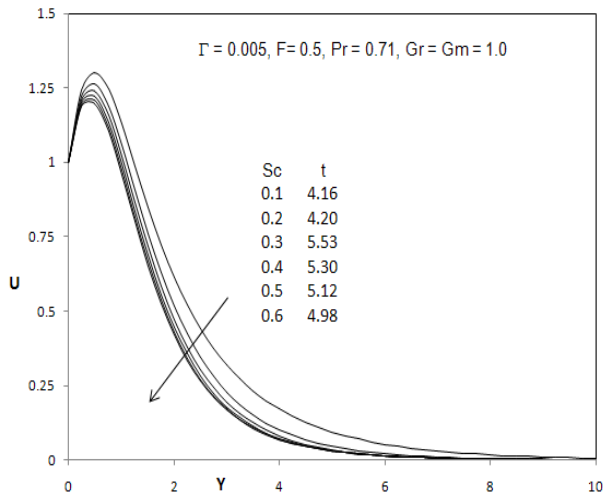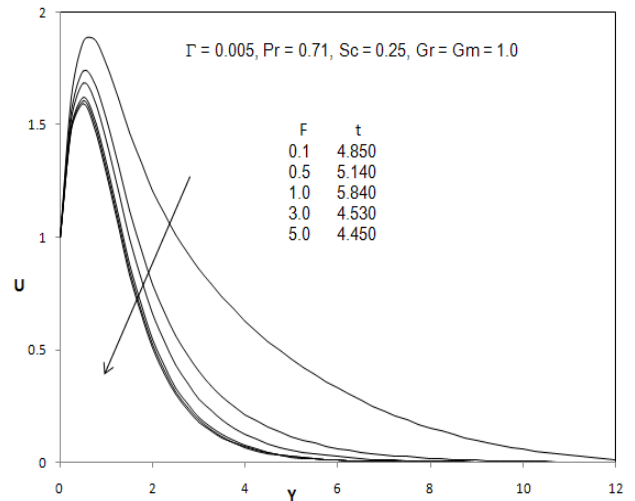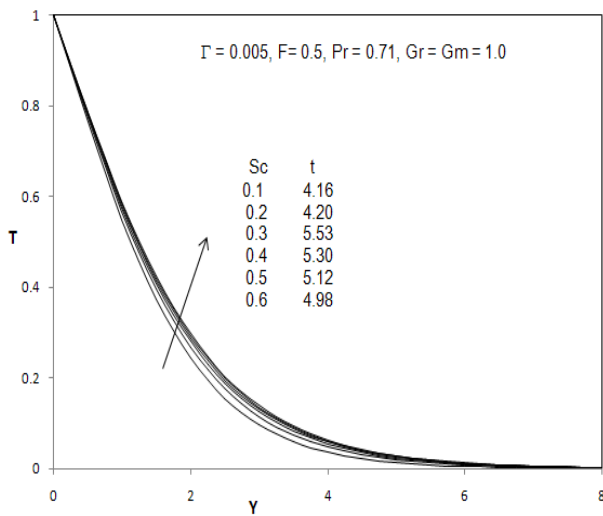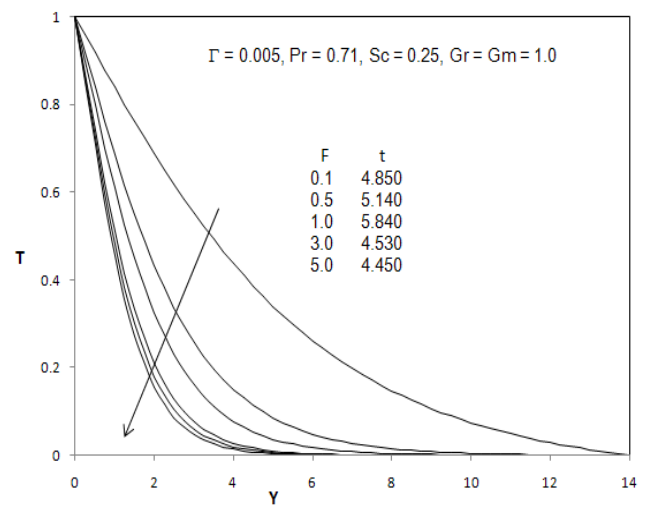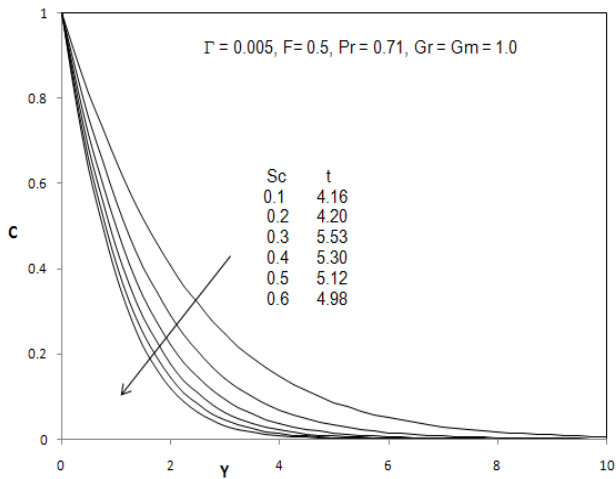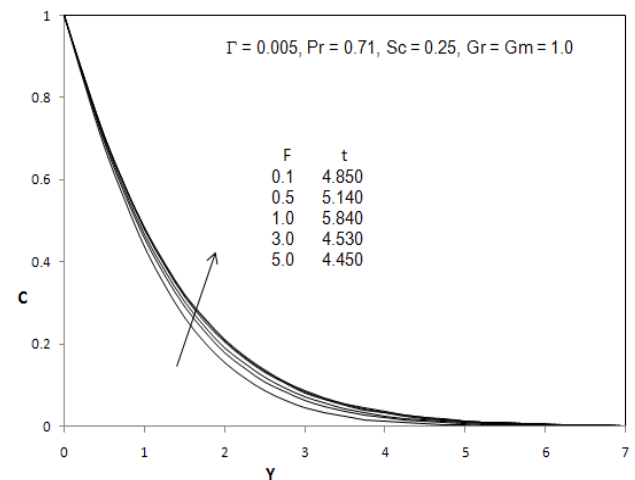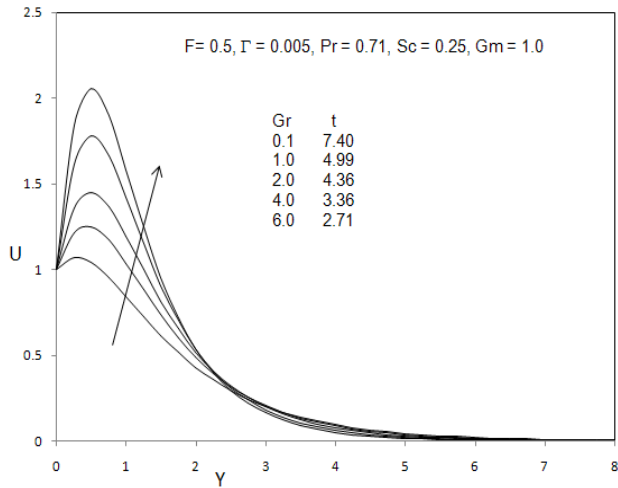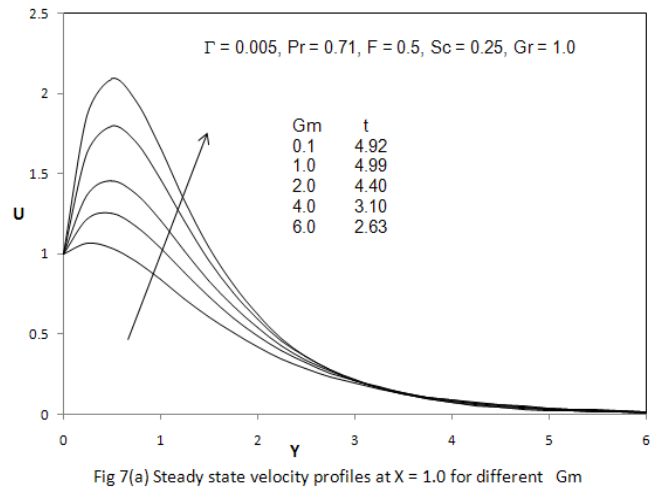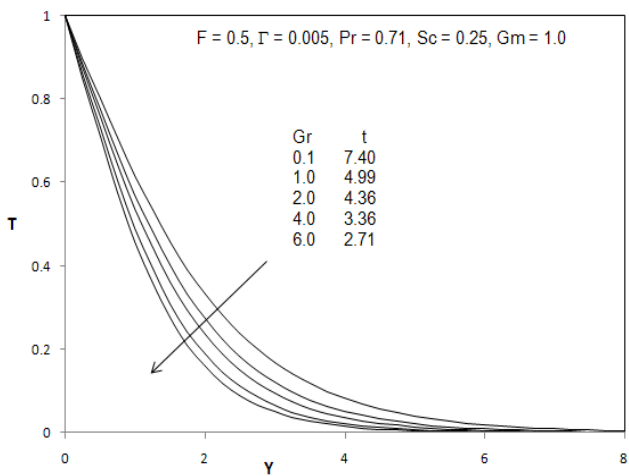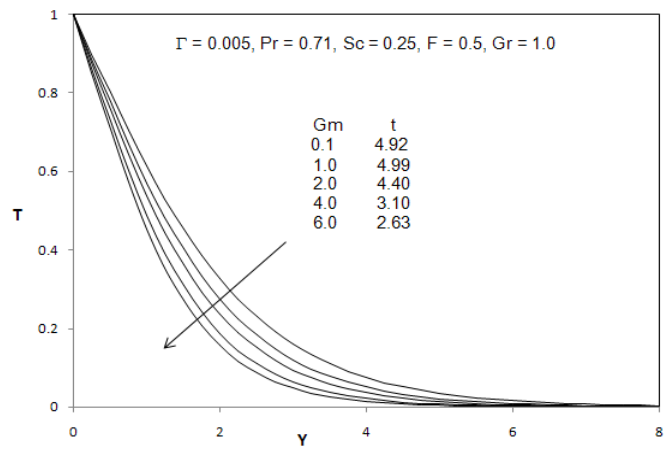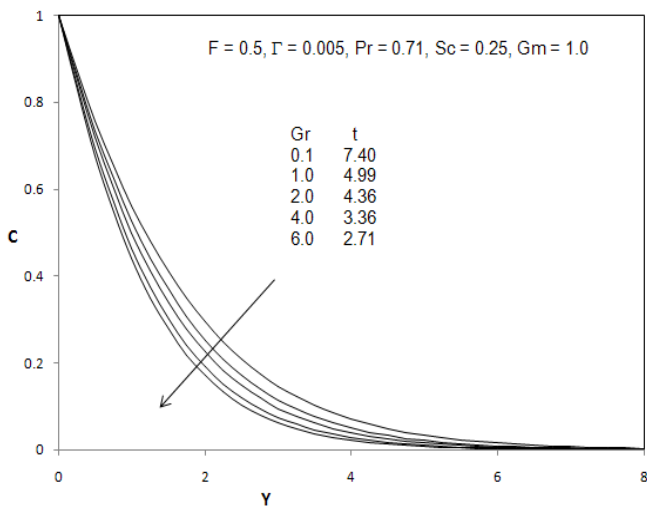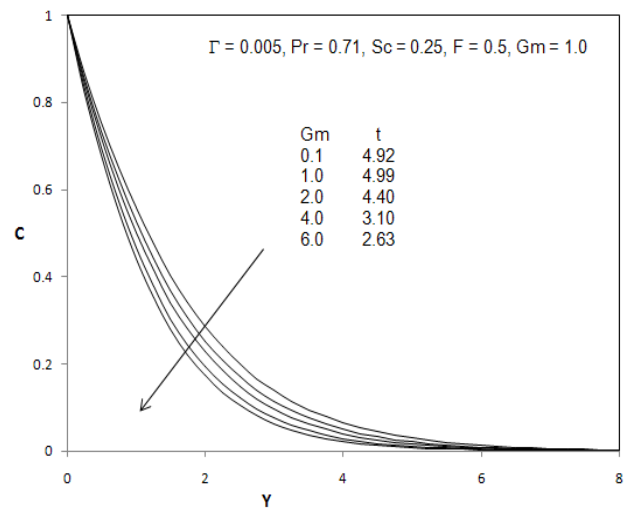Fig 3(c) Steady state concentration profiles at X = 1.0 for different Pr

Fig 4(a) Steady state velocity profiles at X = 1.0 for different Sc

Fig 5(a) Steady state velocity profiles at X = 1.0 for different F

Fig 4(b) Steady state temperature profiles at X = 1.0 for different Sc

Fig 5(b) Steady state temperature profiles at X = 1.0 for different F

Fig 4(c) Steady state concentration profiles at X = 1.0 for different Sc

Fig 5(c) Steady state concentration profiles at X = 1.0 for different F

Fig 6(a) Steady state velocity profiles at X = 1.0 for different Gr

Fig 7(a) Steady state velocity profiles at X = 1.0 for different Gm

Fig 6(b) Steady state temparature profiles at X = 1.0 for different Gr

Fig 7(b) Steady state temparature profiles at X = 1.0 for different Gm

Fig 6(c) Steady state concentration profiles at X = 1.0 for different Gr

Fig 7(c) Steady state concentration profiles at X = 1.0 for different Gm
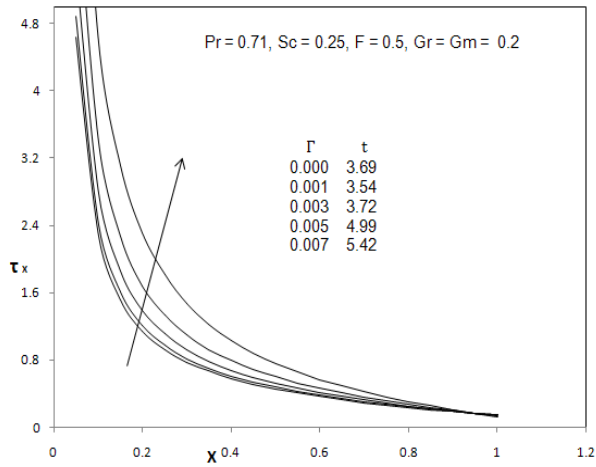
Fig 8(a) The local Skin friction results for different Γ
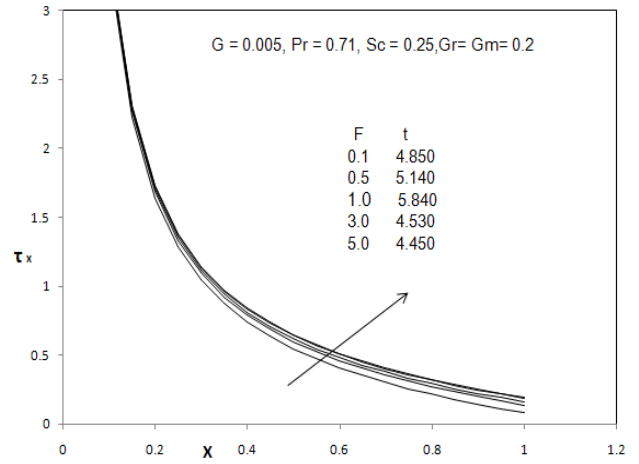
Fig 9(a) The local Skin friction results for different F
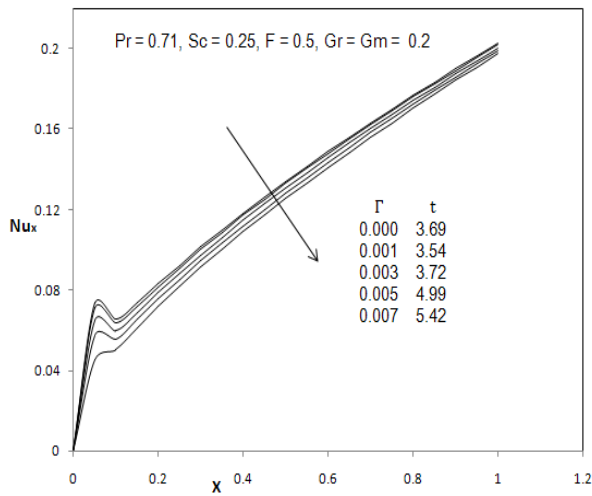
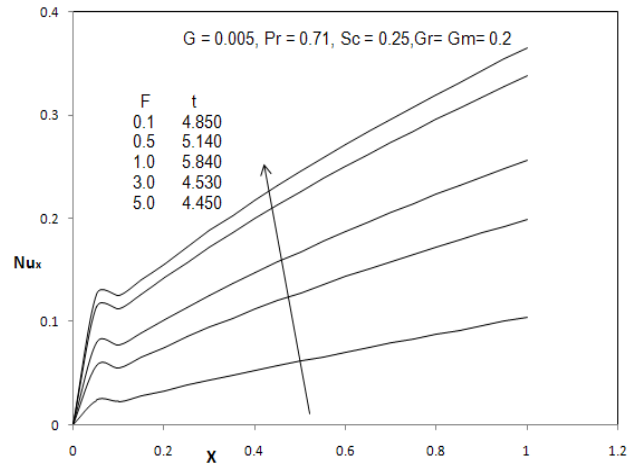Fig 8(b) the local Nusselt number results for different Γ

Fig 9(b) The local Nussult number results for different F
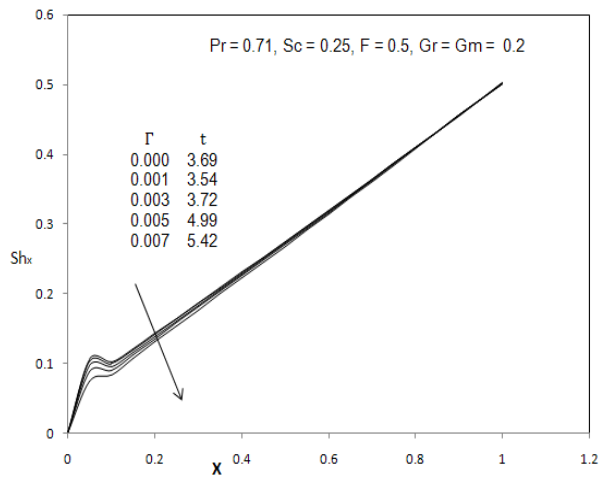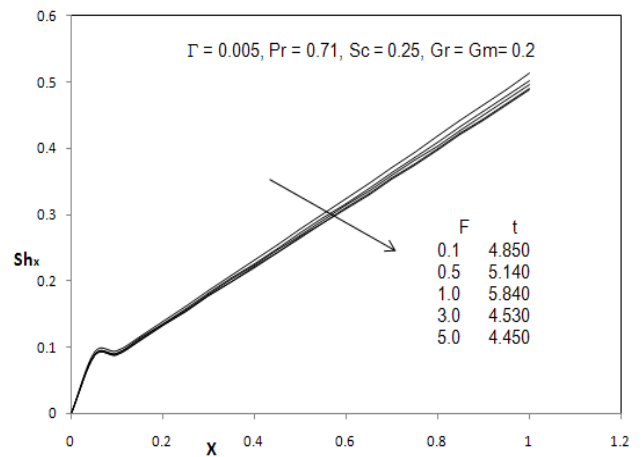

Fig 8(c) the local Sherwood number results for different Γ

Fig 9(c) the local Sherwood number results for different F